Available online at www.sciencedirect.com

ScienceDirect

Journal of Crystal Growth 310 (2008) 1614–1618

JOURNAL OF CRYSTAL GROWTH

www.elsevier.com/locate/jcrysgro

Non-polar *a*-plane GaN grown on $LaAlO_3$ (0 0 1) substrate by pulsed laser deposition

Yen-Teng Ho[a,*], Mei-Hui Liang[b], Feng-Ke Hsiao[c], Wei-Lin Wang[a], Chun-Yen Peng[a], Wei-Da Chen[a], Wei-I Lee[c], Li Chang[a,*]

[a] *Department of Materials Science and Engineering, National Chiao Tung University, 1001, Tahsueh Road, Hsinchu 300, Taiwan, ROC*
[b] *Center of General Education, Chung Hua University, Hsinchu, Taiwan, ROC*
[c] *Department of Electrophysics, National Chiao Tung University, Hsinchu, Taiwan, ROC*

Abstract

Non-polar $(1\,1\,\bar{2}\,0)$ GaN has been successfully grown on (0 0 1) $LaAlO_3$ (LAO) substrate by pulsed laser deposition method. The nitrogen plasma is essential to grow pure *a*-plane GaN films. The insertion of a ZnO buffer layer improves the quality of GaN thin film as shown by X-ray diffraction. Reflection high energy electron diffraction and cross-sectional transmission electron microscopy with selected area diffraction reveal two types of *a*-plane GaN domains perpendicular to each other in orientation relationships of $[0\,0\,0\,1]_{GaN} \| [1\,\bar{1}\,0]_{LAO}$ and $[1\,\bar{1}\,00]_{GaN} \| [1\,\bar{1}\,0]_{LAO}$.

PACS: 61.10.Nz; 68.37.−d; 68.37.Lp; 81.15.Fg

Keywords: A1. X-ray diffraction; A3. Laser epitaxy; B1. Nitride

1. Introduction

GaN and related III–V nitrides have attracted much attention in the past decade due to their successful incorporation into white light and ultraviolet light-emitting diodes, blue light laser diodes, and high power devices. The GaN in these devices is mainly grown in the direction parallel to [0 0 0 1]*c*-axis. The optoelectronic devices of *c*-plane GaN suffer from undesirable spontaneous and piezoelectric polarization effects, which greatly affect the carrier recombination lifetime and quantum efficiency. To avoid the so-called quantum confined Stark effect in nitride-based optical devices, growth of high-quality GaN films with non-polar surface such as *m* and *a*-planes has been intensively studied in recent years. The most commonly used substrate nowadays for *a*-plane $(1\,1\,\bar{2}\,0)$ GaN growth is *r*-plane sapphire. However, the large lattice mismatch (>16%) between GaN and sapphire in the $[1\,\bar{1}\,0\,0]$ direction may result in a high density of dislocations in the GaN films [1]. Growth of *a*-plane GaN on a suitable substrate with smaller lattice mismatch may have better quality films.

$LaAlO_3$ (LAO) has a rhombohedral structure at room temperature, but it can be regarded as pseudocubic with lattice constant of 3.79 Å. It has been widely used as substrate for oxide thin film growth. From the dimensions of GaN and LAO unit cells, the lattice mismatch of LAO (0 0 1) with *c*-plane GaN is estimated to be less than 3% [2]. Growth of GaN on LAO substrate using molecular beam epitaxy (MBE) method has been reported, showing that only *c*-plane wurtzite GaN films are obtained [2,3].

Pulsed laser deposition (PLD) method has been demonstrated as a useful technique to grow high-quality GaN films at low temperature [4–8]. In this study, we show the growth of non-polar $(1\,1\,\bar{2}\,0)$ GaN thin films on (0 0 1) LAO substrates by PLD. The effects of nitrogen gas and ZnO buffer on GaN qualities were also studied using X-ray diffraction (XRD), reflected high energy electron diffraction (RHEED), and transmission electron microscopy (TEM).

---

*Corresponding authors. Tel.: +886 3 5731615; fax: +886 3 5724727.
E-mail address: chia500@yahoo.com.tw (L. Chang).

0022-0248/$ - see front matter © 2007 Elsevier B.V. All rights reserved.
doi:10.1016/j.jcrysgro.2007.11.047

2. Experimental procedure

The growth of GaN and ZnO films were performed in a DCA PLD500 PLD system using a pulsed KrF-excimer laser of 248 nm wavelength and 25 ns duration under a base pressure of 1×10^{-8} Torr. Both ZnO and GaN ablation targets in diameter of 2 inch were loaded in the PLD system. The ZnO target was prepared by pressing and sintering of single phase ZnO powder of 4 N purity, while the GaN target was a poly-crystal disk manufactured by hydride vapor-phase epitaxy method. After cleaning in boiled acetone and isopryl alcohol, a 2 inch diameter LAO (0 0 1) substrate was transferred into the PLD chamber. In this study, the substrate temperature was set at 750 °C. For the study of the nitrogen effect, a number of GaN growth runs were performed with N_2 (5 N purity) only, while some experiments were done using electron cyclotron resonance (ECR) plasma for N_2 treatment. The partial pressure of nitrogen was kept at 20 m Torr. Also, GaN growth on a ZnO buffer layer deposited on LAO was done with the ECR plasma condition for nitrogen treatment. For growth of the ZnO buffer layer, the oxygen with 5 N purity was introduced into the chamber with partial pressure of 20 m Torr. The KrF laser power density was set to 1–2 J/cm^2 with 3 Hz repetition frequency for ablation of GaN and ZnO targets. To monitor the surface morphology in different growth stages, RHEED patterns were taken from an Oxford Scientific OS-RHEED system operated at 15 kV. The crystallinity of GaN thin films was examined using a Bruker D8 X-ray diffractometer. TEM in cross section was carried out in a FEI Tecnai 20 microscope and a JEOL 2010F microscope to investigate the microstructure of $(1\,1\,\bar{2}\,0)$ GaN thin films on LAO.

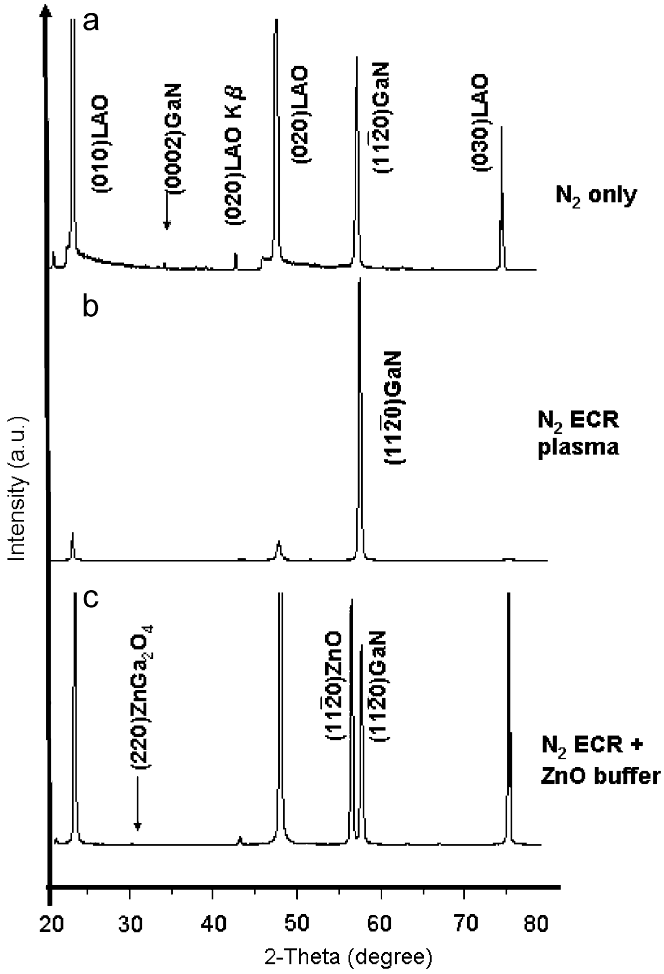

Fig. 1. X-ray diffraction 2θ profiles of GaN samples grown with N_2 gas (a), ECR plasma (b), and ZnO buffer (c) on LAO substrates.

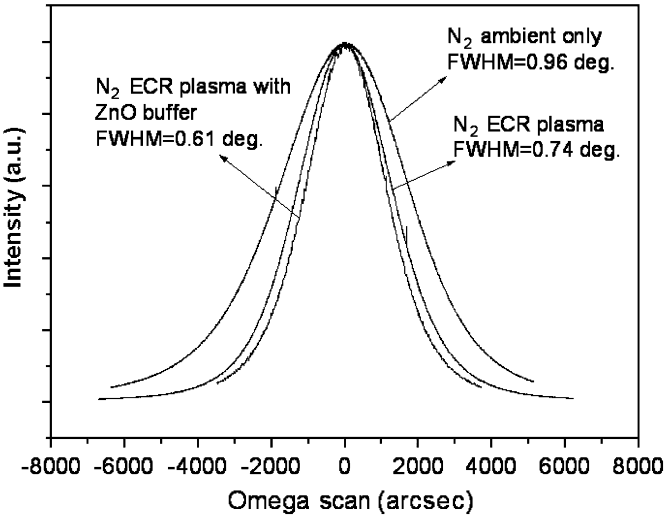

Fig. 2. $(1\,1\,\bar{2}\,0)$ X-ray rocking curve plots of GaN grown by different conditions.

3. Results and discussion

Fig. 1 plots X-ray θ–2θ profiles of GaN films grown on LAO with different deposition conditions. As can be seen, all the samples show strong $(1\,1\,\bar{2}\,0)$ reflection of GaN. Only the sample grown under the N_2 ambient exhibits a minor peak of (0 0 0 2) GaN as shown in Fig. 1(a). Thus, the plasma treatment of nitrogen gas seems favorable for the formation of *a*-plane GaN. The $(1\,1\,\bar{2}\,0)$ X-ray rocking curves of these samples are shown in Fig. 2. The full width at half maximum (FWHM) of the curve is larger for the N_2 sample (0.96°) than for the plasma sample (0.74°). It is clear that the crystalline quality of GaN grown with the ECR nitrogen plasma is improved in comparison with that grown with N_2. For GaN growth on ZnO buffered templates on LAO, it is noticed that both GaN and ZnO have *a*-plane reflections in Fig. 1(c), implying that GaN and ZnO have a close lattice relationship [9,10]. In addition, there is a minor peak identified as (2 2 0) of $ZnGa_2O_4$ which may be due to an interfacial layer formed between GaN and ZnO. The FWHM of $(1\,1\,\bar{2}\,0)$ X-ray rocking curve from a ZnO buffer with the same ECR plasma treatment for N_2 used for direct growth of GaN on LAO is reduced to 0.61°(Fig. 2), suggesting that ZnO buffer improves the structural quality of GaN as well.

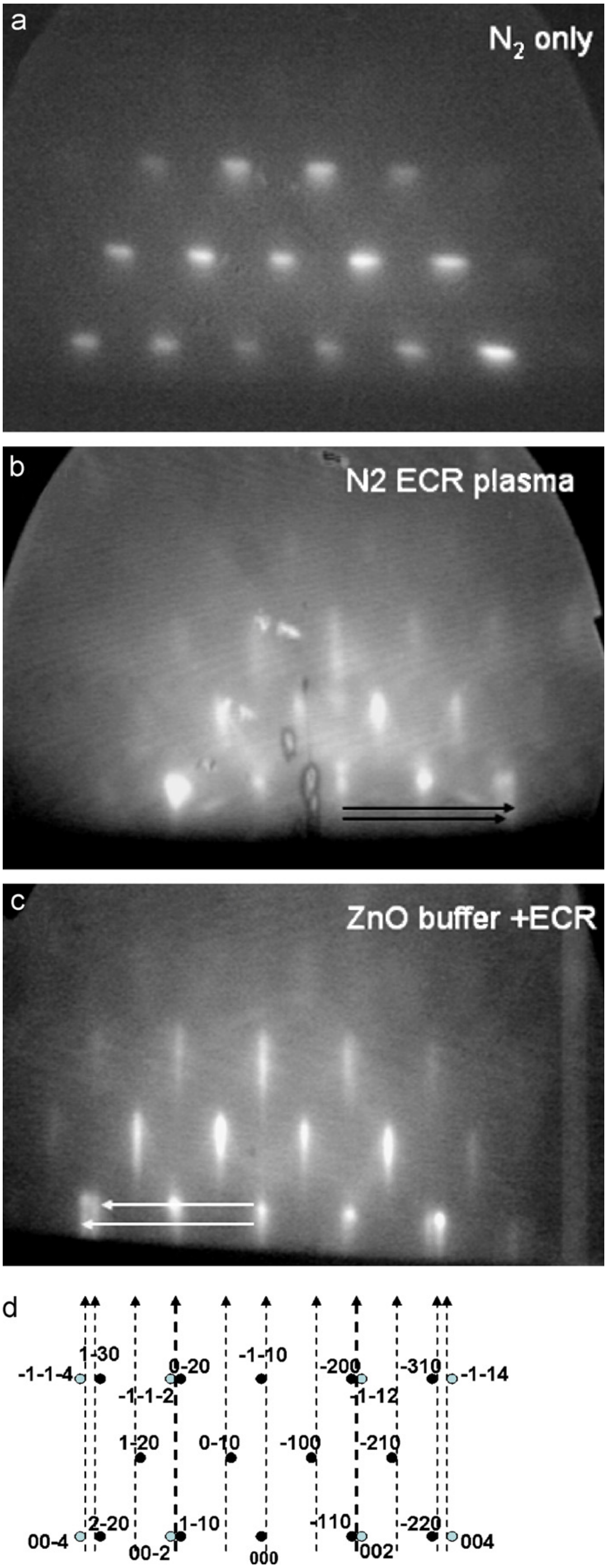

Fig. 3. RHEED patterns of GaN films along [1 1 0] LAO. (a) The GaN deposited on LAO only with N_2, (b) with N_2 ECR plasma, and (c) ZnO buffer layer. (d) Schematic drawing of $[0\,0\,0\,1]_{\mathrm{GaN}}$ and $[0\,1\,\bar{1}\,0]_{\mathrm{GaN}}$ zone-axis patterns. The dash lines are corresponding to the positions of reflections in the RHEED patterns.

Fig. 3 shows RHEED patterns of GaN grown on LAO substrates using different growth parameters. The incident azimuth of the electron beam is along [1 1 0] of LAO substrate. Fig. 3(a) is the RHEED pattern of a GaN film deposited in N_2 ambient. The spotty pattern indicates a 3D growth mode for GaN deposition. As shown in Fig. 3(b), the RHEED pattern of GaN grown with the ECR nitrogen plasma exhibits streaky lines, suggesting that the surface smoothness of GaN is improved. The RHEED pattern of GaN deposited on the ZnO/LAO template in Fig. 2(c) shows sharp streaky lines, which suggests further improvement of the film quality and surface smoothness of GaN. In Figs. 2(b) and (c), it can be seen that there are two periods of line spacing as indicated by the arrows in the patterns. Fig. 3(d) shows a schematic diagram in which the reflections in the RHEED pattern are indexed as in $[0\,0\,0\,1]_{\mathrm{GaN}}$ and $[0\,1\,\bar{1}\,0]_{\mathrm{GaN}}$ zone-axis patterns. Furthermore, the RHEED patterns taken with rotation of every 90° azimuthal angle reveal the same characteristic diffraction features, indicating that there exists four-fold symmetry for the *a*-plane GaN films. To interpret the observations, we suggest that there exist two kinds of growth domains perpendicular to each other in $(1\,1\,\bar{2}\,0)$ GaN on LAO.

To further confirm the above results, cross-sectional TEM was performed. Fig. 4 shows a selected-area diffraction (SAD) pattern from GaN on (0 0 1) LAO with the ECR nitrogen plasma treatment. Obviously, the diffraction spots can be indexed as two GaN diffraction zone axes patterns in $[1\,\bar{1}\,0\,0]$ and [0 0 0 1] as shown in Fig. 3(d). From the SAD, two orientation relationships can be deduced as $[0\,0\,0\,1]_{\mathrm{GaN}} \| [1\,1\,0]_{\mathrm{LAO}}$ and $[1\,\bar{1}\,0\,0]_{\mathrm{GaN}} \| [1\,1\,0]_{\mathrm{LAO}}$, which correspond to the two types of *a*-plane GaN growth domains on LAO.

Fig. 5 shows bright field and dark field TEM micrographs of $(1\,1\,\bar{2}\,0)$ GaN grown on (0 0 1) LAO without/with ZnO buffer layer in the same ECR plasma condition. These images are taken under the two-beam diffraction condition of $g = [1\,0\,\bar{1}\,0]$. Fig. 5(a) shows that the film thickness of GaN is about 260 nm, giving the corresponding deposition rate about 0.4 Å/pulse. The interface between GaN and LAO is abrupt. The dark field TEM micrograph in Fig. 5(b) exhibits bright and dark image contrast in the GaN film, suggesting that two differently orientated grains exist in the film with the average grain size of 120 nm. Fig. 5(c) and (d) are bright field/ dark field TEM micrographs of GaN grown on ZnO buffer layer. Fig. 5(c) shows that the interface between GaN and ZnO is sharp. The thickness of GaN and ZnO buffer layer is estimated as 210 and 180 nm, respectively. The dark field image in Fig. 5(d) also shows two different orientation contrast which extends from ZnO to GaN across their interface. Hence, it is believed that GaN growth follows the microstructure of ZnO template on LAO substrate. Fig. 6 shows a high-resolution TEM image of the GaN/LAO interface. No interlayer between GaN and LAO can be seen in the image, indicating that no reaction occurs between them. Also, lattice fringes with the fast-Fourier-transform patterns in the insets illustrate that both orthogonal GaN domains coexist on LAO.

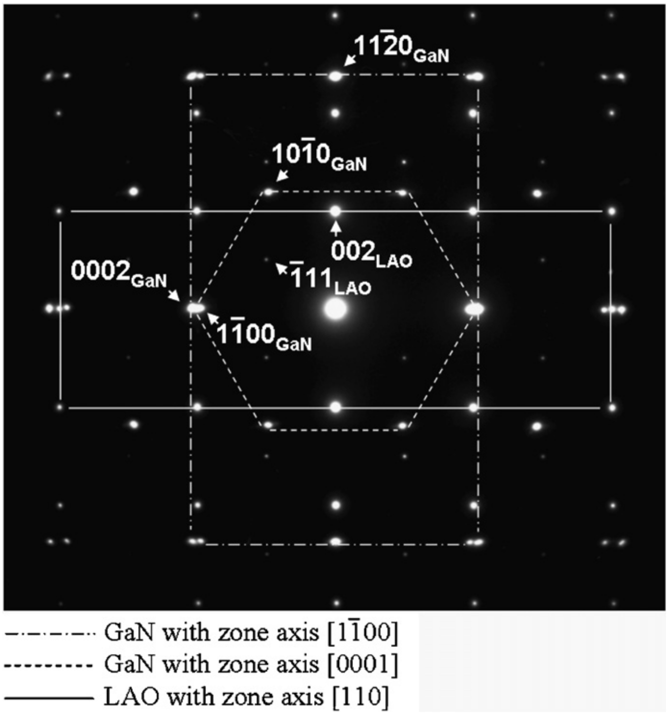

Fig. 4. Selected-area diffraction pattern of GaN grown on $(1\,0\,0)_{LAO}$ substrate in $[1\,1\,0]_{LAO}$ zone axis. Two sets of diffraction patterns from $[0\,0\,0\,1]_{GaN}$ and $[1\,\bar{1}\,0\,0]_{GaN}$ are shown in broken lines.

As shown above, both GaN and ZnO of wurtzite structure can be grown on LAO. From the orientation relationships and crystallography of *a*-plane GaN and LAO (0 0 1), therefore, it can be shown that the LAO has a repeated distance of 5.36 Å along $\langle 1\,1\,0\rangle$; which can closely match with GaN of 5.18 Å along *c*-axis and 5.52 Å ($\sqrt{3}a_{GaN}$) along *m*-axis. Hence, the two oriented growth modes for deposition of *a*-plane GaN is simply due to cubic symmetry of LAO (0 0 1).

4. Conclusions

We demonstrate that pure non-polar *a*-plane $(1\,1\,\bar{2}\,0)$ GaN films can be grown on (0 0 1) LAO by PLD. Using the ECR nitrogen plasma source and insertion of ZnO buffer layer improves film quality of *a*-plane GaN.

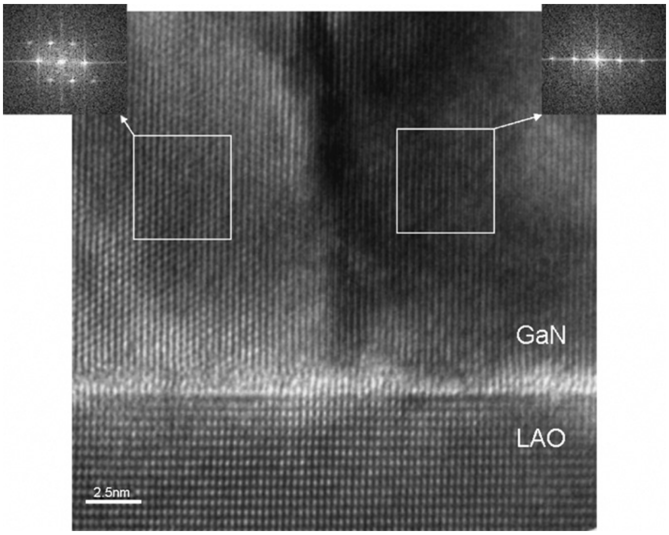

Fig. 6. High-resolution TEM image of GaN grown on LAO. The insets are FFT diffraction patterns from the framed *a*-plane GaN regions in [0 0 0 1] and $[1\,\bar{1}\,0\,0]$ zone axes.

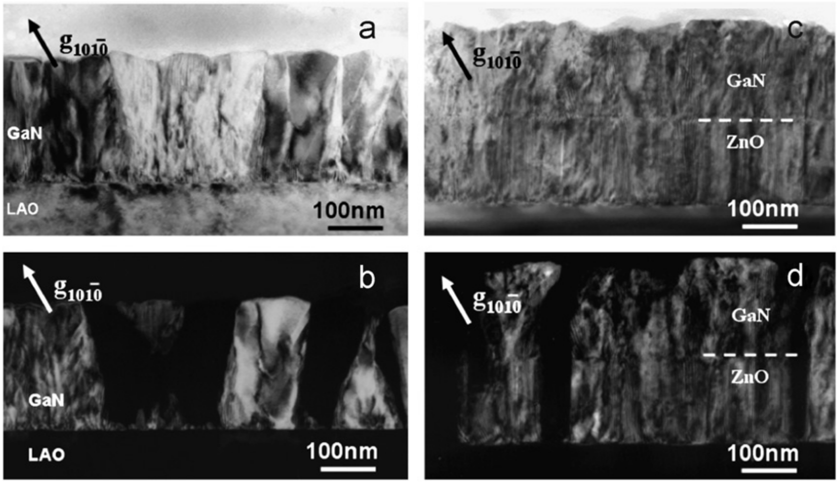

Fig. 5. (a) Bright field and (b) dark field cross-sectional TEM images of GaN grown on LAO. (c) Bright field and (d) dark field cross-sectional TEM images of GaN grown on LAO with insertion of ZnO buffer layer.

Moreover, RHEED and TEM with SAD show two orientation relationships as $(1\,1\,\bar{2}\,0)_{\mathrm{GaN}} \| (0\,0\,1)_{\mathrm{LAO}}$, and $[0\,0\,0\,1]_{\mathrm{GaN}} \| [1\,\bar{1}\,0]_{\mathrm{LAO}}$ and $[1\,\bar{1}\,0\,0]_{\mathrm{GaN}} \| [1\,\bar{1}\,0]_{\mathrm{LAO}}$. Hence, growth of $(1\,1\,\bar{2}\,0)$ GaN film on $(1\,0\,0)$ LAO forms two types of *a*-plane GaN domains perpendicular to each other as a result of LAO cubic symmetry.

Acknowledgment

Part of this work was supported by National Science Council and Ministry of Education, Taiwan, ROC.

References

[1] R. Kroger, T. Paskova, S. Figge, D. Hommel, A. Rosenauer, B. Monemar, Appl. Phys. Lett. 90 (2007) 081918.
[2] J.J. Lee, K.Y. Kang, Y.S. Park, C.S. Yang, H.S. Kim, K.H. Kim, T.W. Kang, S.H. Park, J.Y. Lee, Jpn. J. Appl. Phys. 38 (1999) 6487.
[3] J.J. Lee, Y.S. Park, C.S. Yang, H.S. Kim, K.H. Kim, K.Y. Kang, T.W. Kang, S.H. Park, J.Y. Lee, J. Crystal Growth 213 (2000) 33.
[4] P. Sanguino, M. Niehus, L. Melo, R. Schwarz, A. Fedorov, J.M.G. Martinho, M.J. Soares, T. Monteiro, Physica B 340–342 (2003) 457.
[5] M. Niehus, P. Sanguino, T. Monteiro, M.J. Soares, E. Pereira, M. Vieira, S. Koynov, R. Schwarz, Solid State Electron. 47 (2003) 569.
[6] Y. Tsuchiya, A. Kobayashi, J. Ohta, H. Fujioka, M. Oshima, J. Crystal Growth 293 (2006) 22.
[7] G. Li, J. Ohta, A. Kobayashi, H. Fujioka, Semicond. Sci. Technol. 21 (2006) 1026.
[8] Y. Tsuchiya, M. Oshima, A. Kobayashi, J. Ohta, H. Fujioka, J. Vac. Sci. Technol. A 24 (2006) 2021.
[9] C.Y. Man, H. Zhung, X. Wei, M. Liu, C.S. Xue, Jpn. J. Appl. Phys. 46 (2) (2007) 526.
[10] B.Y. Man, C. Yang, H.Z. Zhuang, M. Liu, X.Q. Wei, H.C. Zhu, C.S. Xue, J. Appl. Phys. 101 (2007) 093519.